

# *EavesDroid*: Eavesdropping User Behaviors via OS Side-Channels on Smartphones

Quancheng Wang<sup>1</sup>, Ming Tang<sup>1\*</sup> and Jianming Fu<sup>1</sup>

**Abstract**—As the Internet of Things (IoT) continues to evolve, smartphones have become essential components of IoT systems. However, with the increasing amount of personal information stored on smartphones, user privacy is at risk of being compromised by malicious attackers. Although malware detection engines are commonly installed on smartphones against these attacks, attacks that can evade these defenses may still emerge.

In this paper, we analyze the return values of system calls on Android smartphones and find two never-disclosed vulnerable return values that can leak fine-grained user behaviors. Based on this observation, we present *EavesDroid*, an application-embedded side-channel attack on Android smartphones that allows unprivileged attackers to accurately identify fine-grained user behaviors (e.g., viewing messages and playing videos) via on-screen operations. Our attack relies on the correlation between user behaviors and the return values associated with hardware and system resources. While this attack is challenging since these return values are susceptible to fluctuation and misalignment caused by many factors, we show that attackers can eavesdrop on fine-grained user behaviors using a CNN-GRU classification model that adopts min-max normalization and multiple return value fusion. Our experiments on different models and versions of Android smartphones demonstrate that *EavesDroid* can achieve 98% and 86% inference accuracy for 17 classes of user behaviors in the test set and real-world settings, highlighting the risk of our attack on user privacy. Finally, we recommend effective malware detection, carefully designed obfuscation methods, or restrictions on reading vulnerable return values to mitigate this attack.

**Index Terms**—Mobile Security, Side-Channel, Behavior Inference, Neural Network.

## I. INTRODUCTION

SMARTPHONES are essential in the Internet of Things (IoT) systems and contain large amounts of sensitive data. In recent years, malicious attacks on these sensitive data have attracted widespread attention. Although the Android system incorporates several security mechanisms to ensure the confidentiality of user privacy, there are still vulnerabilities that attackers can exploit to steal sensitive data from smartphones, such as side-channel attacks [1] and physical layer attacks [2].

Side-channel attacks allow attackers to infer sensitive information by monitoring some affected states or attributes without high-level privileges. Until now, researchers have discovered a

variety of side-channel attacks against Android smartphones. For example, CPU caches can provide the cache contention state between different applications and leak sensitive information such as user keystrokes [3]. Then, GPU performance counters [4] related to graphics rendering can leak security-critical inputs from users. Moreover, graphics interrupts [5] can represent unique characteristics of the GPU workload and provide information about smartphone user behaviors. In addition, gyroscopes [6] and accelerometers [7] interfered with by speakers playing audio can provide sensitive information such as speech authentication PINs.

Besides CPU [3], [8]–[10], GPU [4], [5], [10]–[12], and IMU sensors [6], [7], [13], many other shared smartphone resources could be potential sources of side-channel attacks [14]–[17]. Among them, the OS kernel is considered an effective target for side-channel attacks, as it provides various system calls for applications to interact with the kernel and can obtain information about the system state (e.g., memory, filesystem, and network). ASVAAN [18] is an OS side-channel attack on Android smartphones that discloses eight vulnerable return values of system calls and can infer application launching and website browsing with an accuracy of 73% and 85% through the DTW algorithm and the k-fold cross-validation.

However, this attack cannot identify more fine-grained user behaviors, which are the on-screen operations that users perform on specific applications by tapping, swiping, scrolling, and other gestures. These finer-grained user behaviors can also be used for further attacks to cause more privacy leakage. For example, by inferring the fine-grained user behaviors, the attacker can obtain the sequence of behaviors of the victim users and then track the habits and preferences of smartphone users to build their profiles or de-anonymize users in the network to infer their locations and identities [19].

To address the limitations of previous work, it is necessary to investigate whether OS side-channel attacks can threaten fine-grained user behaviors on smartphones. Therefore, in this paper, we first analyze the correlation between the vulnerable return values of system calls found in previous work [18] and fine-grained user behaviors and find that the return values can provide privacy about fine-grained user behaviors. We then conduct a comprehensive analysis of all system calls in the Android system and finally find two new vulnerable return values not considered in the previous work: `statvfs.f_ffree` and `sysinfo.freeram`, where the former is the most effective return value in inferring fine-grained user behaviors.

After exploring all the vulnerable return values, we present *EavesDroid*, an application-embedded OS side-channel attack on smartphones that enables unprivileged attackers to infer

Manuscript received March 7, 2023; revised July 12, 2023; accepted July 13, 2023.

Q. Wang, M. Tang, J. Fu are with the Key Laboratory of Aerospace Information Security and Trusted Computing, Ministry of Education, School of Cyber Science and Engineering, Wuhan University, Wuhan 430072, China. Email: wangquancheng@whu.edu.cn, m.tang@126.com, jmfu@whu.edu.cn

\*Corresponding author: Ming Tang.

Copyright (c) 20xx IEEE. Personal use of this material is permitted. However, permission to use this material for any other purposes must be obtained from the IEEE by sending a request to pubs-permissions@ieee.org.

fine-grained user behaviors accurately. Our attack exploits the correlation between these behaviors and the return values of system calls. To carry out the attack, We develop a malicious service that can be widely deployed on different models and versions of Android smartphones. This service reads vulnerable return values by frequently invoking system calls in the background when the user performs fine-grained user behaviors. Finally, the attacker gathers these return values to classify and identify specific user behaviors.

Two significant challenges during the inference process can lead to confusion: each time series collected is misaligned due to different system states at the time of collection; other running processes can cause fluctuations in the return values of system calls. Nevertheless, we demonstrate that *EavesDroid* can address these challenges and seriously threaten fine-grained user behaviors with a new CNN-GRU classification model. Then, we apply min-max normalization to the original time series to align the time series and thus improve inference accuracy. In addition, we combine multiple features of the return values to eliminate the influence of other running processes and further improve inference accuracy.

Afterward, we evaluate *EavesDroid* on different models and versions of Android smartphones. The experimental results show that *EavesDroid* can achieve 98% and 86% inference accuracy for already considered 17 user behaviors in the test set and real-world settings. Moreover, we also validate that our attack can be launched with over 80% accuracy across different device models and application versions. In addition, the experiments also demonstrate that our attack can distinguish 41 multi-behavior time sequences with approximately 89% accuracy and achieve 90% inference accuracy on noisy scenarios, which is sufficient to justify the effectiveness of our attack. Finally, our attack can also bypass existing static and dynamic anti-malware engines, further increasing the vulnerability of our attack.

Furthermore, we also discuss some alleviations for the proposed attack. First, existing detection malware detection methods still leave security holes for attackers to infer fine-grained user behaviors, which urges the emergence of effective detection methods. Second, although obfuscating the vulnerable return values can confuse attackers, there needs a tradeoff between security and performance/resource overhead. Third, a more effective and practical approach is to use access control (such as SELinux) to restrict application privileges from accessing vulnerable return values. We hope that our proposal will be helpful for future research on countermeasures.

**Contribution.** To the best of our knowledge, our work is the first that allows inferring the fine-grained user behaviors via OS side-channel attacks on smartphones. In summary, we make the following contributions:

- We prove that the return values of system calls can be used to infer fine-grained user behaviors and find two new vulnerable return values never disclosed in the previous work after the comprehensive analysis.
- We propose an application-embedded OS side-channel attack on smartphones called *EavesDroid*, allowing an unprivileged attacker to invoke system calls and read vulnerable return values to infer fine-grained user behaviors.

- We introduce a new CNN-GRU network to classify fine-grained user behaviors. Then we apply min-max normalization to the original time series and combine multiple features of return values to improve inference accuracy.

## II. BACKGROUND

In this section, we provide background information and related work regarding side-channel attacks on smartphones, system calls, and deep learning techniques.

### A. Side-Channel Attacks on Smartphones

Side-channel attacks exploit unintended information leakage from computing devices or implementations to infer sensitive information [1]. And software-based side-channel attacks are the most common attacks on mobile devices due to the following reasons. On the one hand, there are numerous shared resources on smartphones, thus attackers can infer sensitive information from the contention state of shared resources, such as CPU, GPU, sensors [20], Java APIs, and procs. On the other hand, attackers can launch their attacks without physically connecting to target devices, and their attack methods can spread through application stores or networks [4].

And researchers have proposed various side-channel attacks on smartphones. The GPU is a potential side-channel leakage source for launching eavesdropping attacks. Yang et al. [4] propose a side-channel attack that exploits GPU rendering overdraw on smartphones. By reading and analyzing performance counters related to GPU rendering, this attack can infer user credentials input with over 80% accuracy on various models of Android smartphones. Graphics interrupts can represent unique features of the GPU workload, allowing spy processes to infer behaviors of other processes. Ma et al. [5] evaluate the potential side-channel of graphics interrupts, the low-level interface between the GPU and the CPU, and shows that graphics interrupts can leak user behaviors with an average accuracy of 88.2%.

IMU sensors are another source of side-channel leakage that can be exploited to compromise user privacy on smartphones. InertiEAR [6] and AccEar [7] are two recent attacks that exploit the IMU sensors to perform acoustic eavesdropping attacks on Android smartphones. InertiEAR uses accelerometers and gyroscopes to eavesdrop on both the top and bottom speakers of smartphones, finally achieving a recognition accuracy of 78.8% and a cross-device accuracy of 49.8% across 12 smartphones. AccEar exploits accelerometer sensors in different scenarios, including different sample rates, audio volumes, and device models, to reconstruct any audio played on a smartphone speaker in an unconstrained vocabulary.

In addition, wired and wireless charging are also used to launch side-channel attacks against smartphones. Charger-Surfing [21] exploits the correlation between the power line activity during charging and the dynamic content on the screen to infer the user's on-screen keystrokes and PIN codes with 92.8% accuracy. Moreover, GhostTalk [22] is another attack that exploits the power line side-channel by launching an inaudible voice command injection attack on smartphones that can fool the human ear and multiple live detection models and

can identify the voice of security-critical information such as passwords and authentication codes with up to 92% accuracy. Furthermore, wireless charging is also a potential source of side-channel leakage, and La et al. [23] propose a side-channel attack that effectively launches a website fingerprinting attack on Android and iOS smartphones with over 90% accuracy by monitoring and analyzing the wireless charger.

### B. Linux System Calls and Deep Learning Techniques

The system calls are the interface between user applications and the Linux kernel. Linux kernel provides its services to applications through system calls, and Linux applications interact with the Linux kernel through APIs formed by a combination of system calls. Moreover, system calls not only help applications perform their functions, but their return values also reflect the state of the computer system. For example, `sysinfo()` [24] returns system statistics, including the number of running processes, the amount of memory available, and the time elapsed since the system booted. Therefore, we can collect time series traces of the system call return values that reflect the system state and infer some information about the running application.

In addition, deep learning [25], [26] is a class of machine learning methods that aims to jointly learn data representations and model parameters from the input dataset. Among the deep learning architectures, convolutional neural networks (CNN) [27] are a class of deep and feed-forward neural networks that perform feature extraction through convolutional and pooling layers. Since time series data formed by a series of data points indexed in time order exist in many application fields, it is an essential research topic to classify time series data with deep learning [28]. In addition, CNN and its variants have been widely applied to time series classification, such as 1d-CNN [29] and MACNN [30]. In our study, we read the return values of system calls that reflect the state of the computer system and convert them into time series traces, then use a customized CNN-GRU network to classify them.

## III. ANALYZING SIDE-CHANNEL VULNERABILITIES IN RETURN VALUES OF SYSTEM CALLS

In this section, we analyze the return values of system calls on smartphones and find that return values can leak fine-grained user behaviors. Moreover, we discover two previously uncovered vulnerable return values that can disclose fine-grained user behaviors through experiments.

### A. Motivation

Previous research has shown that the return values of system calls can leak application launch events and website browsing events [18]. Since identifying fine-grained user behaviors can be used for further attacks to cause more privacy leakage, it is necessary to investigate whether OS side-channel attacks can threaten fine-grained user behaviors on smartphones. On the one hand, the attacker can use fine-grained user behaviors to track the habits and preferences of smartphone users. Then, the attacker can use thousands of habits to build user profiles and

violate user privacy, such as precision marketing to sell products to users, targeted ad delivery, and purposeful intelligence gathering. On the other hand, the attacker can de-anonymize users in the network with fine-grained user behaviors, such as inferring the user's location and identity [19].

Furthermore, we also find that the disclosed vulnerable return values are related to memory and filesystem resources on smartphones. Meanwhile, many other return values are also associated with memory, filesystem, and other resources in the Linux kernel, such as `statvfs.f_ffree` (the number of free blocks). Therefore, it is interesting to explore whether there are undisclosed vulnerable return values that can reveal fine-grained user behaviors.

### B. Leaking User Behaviors through Return Values

As mentioned in Section II, the return values of system calls may reflect the state of the system affected by user behaviors. Hence, we first conduct a preliminary experiment on OPPO K10 using the Telegram application to verify this correlation.

```
extern "C" JNIEXPORT jint JNICALL
Java_com_example_app_DemoService_func (
    JNIEnv *env, jobject this) {
    struct sysinfo info{};
    sysinfo(&info);
    return info.procs;
}
```

Fig. 1. An example of the malicious native code: reading the number of current processes.

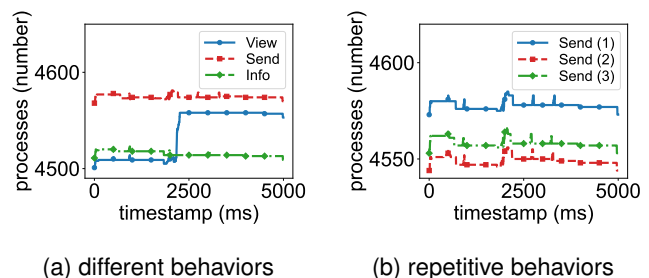


Fig. 2. The return values of `sysinfo.procs` when the user performs different behaviors and repetitive behaviors, where "Send (1)", "Send (2)" and "Send (3)" denotes different instances of "Send".

Fig. 1 shows an example of the malicious native code, where the attacker calls the `sysinfo()` system call and repeatedly reads the number of current processes, then uses this return value to infer fine-grained user behaviors. In the analysis experiments, malicious native code is embedded in our malicious application that always runs in the background of the victim's smartphone. Each time this function executes, the attacker can read this return value to get the number of running processes. With a sampling rate of 1000 samples per second and a sampling time of 5 seconds, the attacker can obtain 5000 data points and use them to generate a time series. The attacker can then repeat this process to gather multiple time series of the same user behavior and different

user behaviors. Finally, the attacker tries to classify these time series and infer the user's behavior.

We then run this experiment and collect the return values of `sysinfo.procs` when the user performs different and repetitive behaviors. As shown in Fig. 2, the line shape of return values varies significantly when the user performs different behaviors, and repetitive user behaviors always result in a similar line shape of return values. Therefore, we can conclude that the return values of system calls can be used to infer user behaviors.

### C. Finding Vulnerable Return Values

Our primary rationale is that if the user performs the same behavior on the smartphone, the change in vulnerable return values should be similar. We calculate the average Euclidean distance between the time series of return values to address their similarity. Suppose  $x$  and  $y$  are two different time series data for a return value, and the length of them is  $T$ , then the Euclidean distance between  $x$  and  $y$  is defined as:

$$d(x, y) = \sqrt{\sum_{i=1}^T (x_i - y_i)^2}. \quad (1)$$

Assuming the return value is  $v$ ,  $N$  is the number of time series data, and  $v[i]$ ,  $v[j]$  represents the  $i$ -th,  $j$ -th time series data of  $v$ , then we define the average Euclidean distance of  $v$  as:

$$avg\_d(v) = \frac{2}{N * (N - 1)} \sum_{i=1}^N \sum_{j=i}^N distance(v[i], v[j]). \quad (2)$$

TABLE I

6 MOST VULNERABLE RETURN VALUES ON ANDROID SMARTPHONES

System Call	Return Value	Average Distance
<code>statvfs()</code>	<code>f_ffree</code>	3.2806
<code>statvfs()</code>	<code>f_bavail</code>	4.3761
<code>sysinfo()</code>	<code>freeram</code>	6.9541
<code>sysinfo()</code>	<code>get_avphys_pages</code>	6.9546
<code>sysconf()</code>	<code>_SC_AVPHYS_PAGES</code>	6.9611
<code>sysinfo()</code>	<code>procs</code>	8.7784

Based on the above principle and the average Euclidean distance formula, we analyze the return values of system calls provided in the system call table and repeat launching Telegram 100 times on OPPO K10. Table I shows the 6 most vulnerable return values during our analysis. Apart from the vulnerable return values discovered in previous work, we find two new vulnerable return values that can be used to infer fine-grained user behaviors:

- `statvfs.f_ffree`: returns the number of free inodes in the filesystem;
- `sysinfo.freeram`: returns the amount of available memory in the system.

And the average distance of `statvfs.f_ffree` is the lowest among all the vulnerable return values.

As an example shown in Fig. 3, we invoke these two vulnerable return values of system calls. In Fig. 3 (a) and Fig. 3 (b), the blue line represents the average line shape of

viewing messages in Telegram, and the red line represents the average line shape of sending messages in Telegram. In Fig. 3 (c) and Fig. 3 (d), the blue line and the red line both represent the average line shape of viewing messages in Telegram, where the blue line is the average line shape for the first 50 times, and the red line is the average line shape for the last 50 times. The experimental results show that the line shape of the return values varies significantly for different user behaviors, and repetitive user behaviors always result in a similar line shape of the return values, which is consistent with the experimental results in Fig. 2 and demonstrates the effectiveness of using these two newly disclosed return values to infer user behaviors.

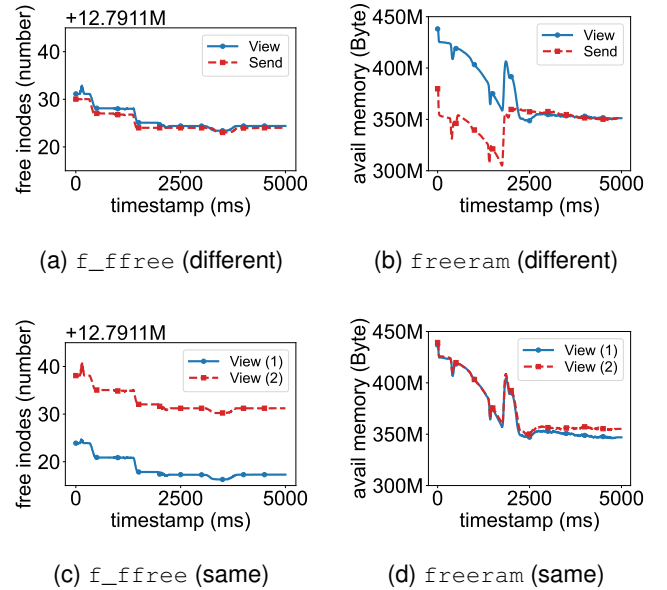


Fig. 3. Newly disclosed system calls used to infer fine-grained user behaviors: `statvfs.f_ffree` and `sysinfo.freeram`, where "View (1)" and "View (2)" denote different instances of "View".

## IV. EAVESDROID ATTACK

In this section, we first introduce our threat model and provide an overview of *EavesDroid*. We then describe the details of accessing return values, gathering device information, and identifying the starting point. Finally, we discuss the implementation scheme of the attack.

### A. Threat Model

**Attack Application.** We assume that our attack application is embedded with malicious code and can be installed and run on the victim's device, which is a reasonable assumption for several reasons. First, the attacker can create a new application that contains malicious code. Since the malicious code only includes legitimate Linux system calls, the malicious application can spread through application stores and evade existing malware detection (see Section VI-G for more details). Second, the attacker can modify an existing application, embed malicious code into it, and then deliver the malicious application to the victim over the Internet. In addition, the malicious application does not need additional

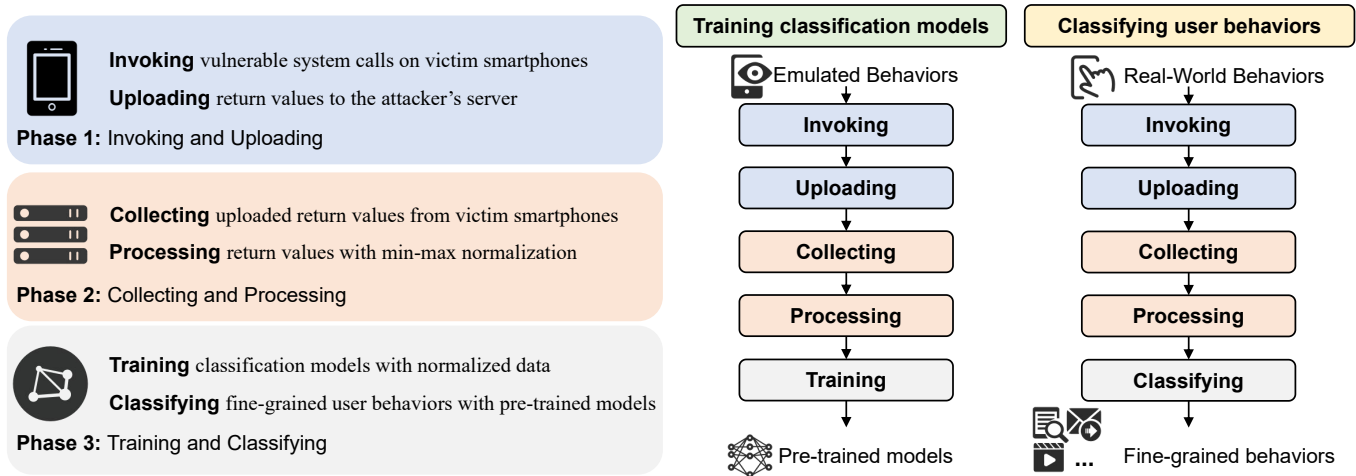


Fig. 4. Overview of *EavesDroid*: invoking and uploading, collecting and processing, training and classifying.

Android permissions to access the return values of Linux system calls, and our attack code runs in the background as an Android service. Therefore, the victim is completely unaware that the malicious application is running.

**Attack Target.** First, our attack targets fine-grained user behaviors on their smartphones, i.e., different user behaviors when using diverse applications, such as viewing messages and sending messages in social applications (e.g., Telegram, Facebook), playing videos and refreshing lists in multimedia applications (e.g., YouTube, Instagram). Second, our attack also targets other information that may violate user privacy, such as whether a PiP hover window is present or background music is playing while the user works on another application.

### B. Attack Overview

As Fig. 4 shows, *EavesDroid* consists of three phases: invoking and uploading, collecting and processing, and training and classifying. Before launching the attack on the victim's smartphone, the attacker emulates user behaviors on devices of different device models and Android versions to collect sufficient training data. These data are used to identify correlations between return values and user behaviors, as well as to build classification models using deep learning techniques.

In the first phase, when the user is using the smartphone, the attacking application silently reads the return values of system calls and device information (including model and Android version) from the victim's smartphone in the background, then uploads the collected data to the attacker's server over the Internet. In the second phase, the attacker collects data uploaded from the malicious application over the Internet for further user behavior identification. Since the raw data collected from smartphones are affected by system states and other factors, resulting in misalignment and fluctuations, the attacker preprocesses the data using mix-max normalization to eliminate the effects. In the third phase, the attacker builds separate classification models for devices of different models and Android versions with the previously emulated user behaviors. Then, the attacker classifies and identifies user

behavior using the data normalized in the second phase and the classification model. In addition, there is no need to retrain the classification model if the data emulated by the attacker remains the same, meaning each classification model only needs to be trained once.

### C. Accessing Return Values and Necessary Information

To launch the attack, we need to read the return values of system calls which can reveal user behaviors, and the device information (model and Android version), which can be used to identify the victim's smartphone. And then, we need to find a method to covertly transmit the collected data to the attacker, and keep our malicious application out of the user's sight.

**Reading.** First, since calling system calls is a pervasive operation in mobile applications and accessible to unprivileged mobile applications, we can use the Android NDK to read the return values of system calls on smartphones. For example, we can get the number of current processes by reading the `procs` field of `sysinfo()`, and obtain the amount of available memory by reading the `freeram` field of `sysinfo()`. Second, to gather information on the device model and Android version for inferring user behaviors, we read the values of `android.os.Build` API directly from the victim's smartphone. We read the values of `manufacturer`, `brand`, and `model` fields to access the information of device model (e.g., "OPPO OPPO PGJM10" for OPPO K10), and the values of `release` and `sdk_int` fields to access the information of Android version (e.g., "12 31" for Android 12). During our attack, the attacking application periodically invokes the system calls to read return values. We read the return values at the speed of 1000 calls per second, and we will further investigate the best reading interval in Section VI-C4.

**Transmitting.** Since using internal storage (e.g., shared preferences) or external storage (e.g., SD card) on smartphones requires the user's authorization, it is not a sound choice to store the collected data on the victim's smartphone (e.g., `/sdcard`) and then send the data to the attacker via the Internet or other communication channels. Nevertheless, the

INTERNET permission is granted by default on the Android system. Whenever the malicious application declares this permission in its manifest file, it can access the Internet without the user's authorization and upload the collected data to the attacker. Then the attacker can use the collected data to infer user behaviors.

**Starting Point.** Another critical issue is to identify the starting point of user behaviors. Our preliminary experiment shows that the return value changes drastically when the user performs a fine-grained behavior (e.g., sending a message), while the return value tends to be stable when the user does not perform any behavior. Based on these observations, we can address the starting point of user behaviors by the following two steps:

- First, we collect the return values of system calls when the user does not perform any behavior, then use the average change as our baseline.
- Then, we compare the return values of system calls to the baseline at other times. If the return value changes significantly from the baseline, we think the user is performing a specific fine-grained behavior at that time.

#### D. Implementation

**Bot Program.** For emulating user behaviors, we implement a bot program in Python for automatic data collection. We simply connect the smartphone to the computer with a USB cable, then use "adb shell" commands to emulate user behaviors. For example, we can use the command "adb shell input tap 100 100" to emulate typing on the screen. And we add random delays between each operation to emulate the varying time interval between user operations for a realistic emulation.

**Android Service.** For the first phase, we implement an Android service in Kotlin to collect the return values of system calls and register the service by modifying the `AndroidManifest.xml` file. In addition, we invoke system calls and read return values using the Android NDK, a native development kit that allows C and C++ code to be used in Android applications. We also use `okhttp3`, a popular third-party web library for Android, to upload the collected data to the server using the HTTP protocol.

**Django.** For the second phase, we implement a web application using Django, an open-source web framework written in Python. We use this web application to collect the data uploaded by the malicious application, and then use the data preprocessing algorithms to eliminate fluctuations and misalignment. We also embed classification models to classify user behaviors into this web application.

**Keras.** For the third phase, we build separate classification models for different devices using Keras, an open-source neural network library written in Python. It allows rapid implementation of deep neural networks and provides user-friendly, modular, and scalable benefits.

### V. A NEW CNN-GRU NETWORK FOR FINE-GRAINED USER BEHAVIOR CLASSIFICATION

In this section, we introduce a new CNN-GRU network for fine-grained user behavior classification. We then use min-max

normalization and multiple feature combinations to eliminate data misalignment and improve inference accuracy.

#### A. The Architecture of the CNN-GRU Network

We use convolutional neural networks (CNN) and gate recurrent neural networks (GRU) to extract features of user behaviors and build classification models. And we also customize the structure and parameters of the CNN-GRU network according to the characteristics of our time series related to user behaviors. Table II summarizes the architecture of the CNN-GRU network, which includes convolutional layers, pooling layers, a GRU layer, a fully connected layer, and an output layer.

There are several reasons why we choose CNN and GRU networks as the basic building blocks of our model:

- First, CNN is the state-of-art solution for extracting features from images and videos [31]. And the data format of our time series representing user behavior is similar to a two-dimensional image, where the x-axis represents the time point while the Y-axis represents the return value of some system call. Therefore, we use CNN to extract features from the time series related to user behaviors.
- Second, GRU is a variant of recurrent neural networks (RNN) for modeling sequential data. The time series associated with user behavior is also a kind of sequential data, where the order and the correlation of the data between each time point are of great significance. Meanwhile, compared with LSTM, GRU has fewer parameters, converges faster, and performs better than LSTM with accuracy guaranteed [32]. Therefore, we choose GRU as the basic building block of our model instead of using only CNN.
- Finally, we also consider the computational complexity of the model. If we only use GRU to model and classify user behaviors, the model will be too complex to result in a slow training process. Therefore, we combine the advantages of CNN and GRU to build the CNN-GRU classification model, while the former can extract features and reduce data dimensionality, and the latter can model sequential data. We will also evaluate the impact of the CNN-GRU network in Section VI-C1.

In the architecture, the input size is  $5000 * n$ , where  $n$  is the number of system calls combined and 5000 is the number of timestamps for each fine-grained user behavior. The input features are first reshaped and extracted with three convolutional layers. In these convolutional layers:

- The number of filters is 64, 128, and 256 for the three convolutional layers.
- The kernel size is 2, the stride is 1, and the padding is the same for each convolutional layer.
- The activation function is *LeakyReLU*, and the leaky ratio is 0.3 for each convolutional layer.
- A max pooling layer with the kernel size 3 and a batch normalization layer are followed by each convolutional layer.

A GRU layer with 128 hidden nodes is then applied to aggregate the features and followed by a fully connected layer.

TABLE II  
THE CNN-GRU ARCHITECTURE FOR CLASSIFYING USER BEHAVIORS

Layer	Input	Parameters	Output
Reshape	(5000, n)	Reshape(10)	(500, n * 10)
Conv_1	(500, n * 10)	Conv(64, 3, leaky_relu) MaxPooling(2) BN	(249, 64)
Conv_2	(249, 64)	Conv(128, 3, leaky_relu) MaxPooling(2) BN	(123, 128)
Conv_3	(123, 128)	Conv(256, 3, leaky_relu) MaxPooling(2) BN	(60, 256)
GRU	(60, 256)	GRU(128) BN	(60, 128)
FC	(60, 128)	FC	(7680)
Output	(7680)	Dense(c, softmax)	(c)

The output of the fully connecting layer is connected to the output layer with the *softmax* activation function, where the number of nodes  $c$  is equal to the number of user behaviors. The network is trained with an ADAM optimizer with a learning rate of 0.001, a sparse categorical cross-entropy loss function, 100 epochs, and a mini-batch size of 32.

During the training process, we first label the emulated data from victim smartphones. Then, we divide the labeled data into training and test sets, which are used to train the network and classify the user behaviors, respectively. The input of the CNN-GRU network is the data preprocessed by the min-max normalization algorithm.

### B. Min-Max Normalization for Eliminating Misalignment

The raw data collected from the smartphones are affected by different system states, leading to data misalignment, which poses a problem for accurate classification.

To solve this problem, we normalize the data using min-max normalization, which is one of the most popular data normalization methods. For each feature of the data, we find the minimum and maximum values of the feature, then set the minimum value to 0 and the maximum value to 1, while every other value is normalized to a decimal between 0 and 1. Consequently, we apply the min-max normalization to the raw time series data to eliminate the misalignment and linearize the data in the range of [0, 1]:

$$x_{i,j}^* = \frac{x_{i,j} - \min_{i=1}^N x_{i,j}}{\max_{i=1}^N x_{i,j} - \min_{i=1}^N x_{i,j}}, \quad (3)$$

where  $x_{i,j}$  is the value of the  $i$ -th time point of the  $j$ -th feature,  $N$  is the number of time points, and  $x_{i,j}^*$  is the normalized value of  $x_{i,j}$ .

Fig. 5 (a) and Fig. 5 (b) show the raw data and the normalized data of `sysinfo.procs` for launching Telegram respectively. Although each time series in the raw data shown in Fig. 5 (a) has similar line shapes, there is still a misalignment that can affect the classification accuracy. Then

the misalignment is eliminated after mix-max normalization as shown in Fig. 5 (b). And we will further investigate the impact of the normalization on the inference accuracy in Section VI-C2.

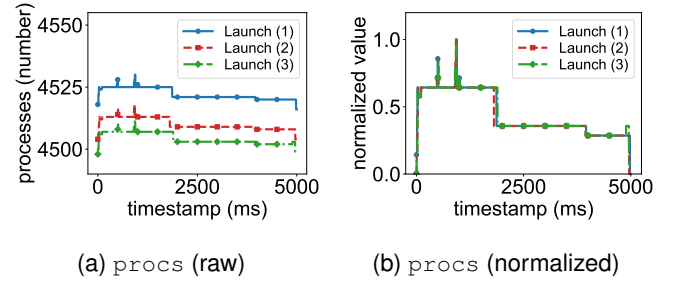


Fig. 5. The difference between the raw data and the normalized data of `sysinfo.procs` for launching Telegram, where "Launch (1)", "Launch (2)" and "Launch (3)" denotes different instances of "Launch".

### C. Multi-Feature Combination for Improving Accuracy

We also realize that there are some different user behaviors, where the line shape of one return value is similar while the line shape of another return value is quite different.

- Let us consider the following two pairs of user behaviors:
- *Launching while a PiP hover window is playing and Launching while a PiP hover window is pausing;*
  - *Launching the Telegram application and Viewing messages in the Telegram application.*

First, for the first pair of user behaviors, as shown in Fig. 6 (a) and Fig. 6 (b), the blue and red lines represent launching Telegram while a PiP hover window is playing and pausing. We cannot distinguish them with `sysinfo.procs` but with `statvfs.f_bavail`. Second, for the second pair of user behaviors, as shown in Fig. 6 (c) and Fig. 6 (d), the blue and red lines represent launching Telegram and viewing messages in Telegram separately. In this case, we can distinguish them with `sysinfo.procs` but cannot distinguish them with `statvfs.f_bavail`. From the above experiments, we can conclude that we cannot fully identify these user behaviors with either `sysinfo.procs` or `statvfs.f_bavail`. But if we combine these two features, the problem is solved.

Therefore, to identify more fine-grained user behaviors and improve classification accuracy, we combine  $n$  different features, so the input size is  $n * t$ , where  $n$  is the number of combined system calls, and  $t$  is the number of time points. And we will further evaluate the impact of feature dimensions on the accuracy in Section VI-C3.

## VI. EVALUATION OF EAVESDROID ATTACK AND CNN-GRU CLASSIFICATION MODEL

We present a thorough analysis and evaluation of our proposed *EavesDroid* attack in this section. First, we describe the experimental setup and evaluate the classification accuracy of 17 categories of user behaviors in a laboratory setting. Second, we have mentioned in previous sections that our customized CNN-GRU neural network contributes to improving inference

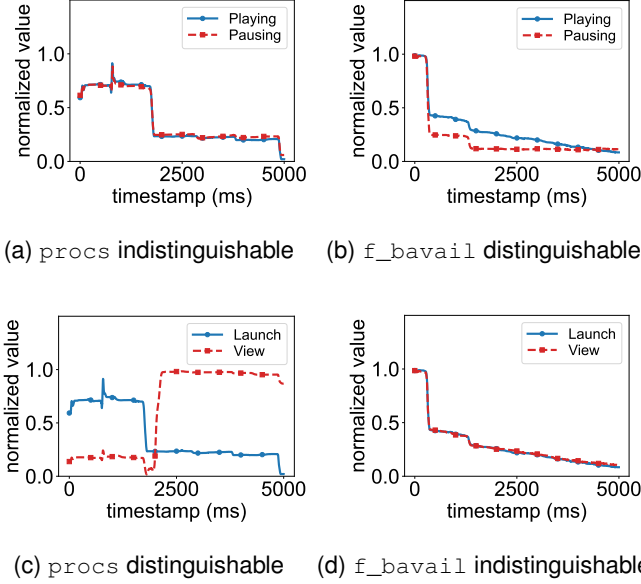


Fig. 6. The line shape of user behaviors cannot be distinguished by only one feature (`sysinfo.procs` or `statvfs.f_bavail`) but can be distinguished by combining these two features.

accuracy. Therefore, we compare the CNN-GRU neural network with the traditional DTW-KNN method and other types of neural networks, compare the different data preprocessing methods, and compare the accuracy with the different number of features to demonstrate the effectiveness of our scheme. Third, since our malicious service needs to continuously read system call return values on the victim’s smartphone and interact with the attacker’s server, it is critical to evaluate how much overhead our attack application imposes on the victim’s smartphone, including power consumption, CPU utilization, memory usage, and network traffic, and whether the classification model can identify user behaviors promptly. So far, all of our evaluations have been conducted on the same smartphone against the identical version of the applications. However, the user may use different devices and different versions of applications, which motivates us to evaluate the adaptability of our attack in such scenarios. In addition, user behaviors in real-world scenarios are not invariant, such as the user may perform multiple operations in the same period. Therefore, we consider three complex cases and evaluate the robustness of such complicated situations. After our systematic and complete analysis in the laboratory setting, we also need to evaluate the inference accuracy for user behaviors in real-world conditions and whether our malicious code can evade the detection by existing anti-malware suites.

#### A. Experimental Setup

**Devices.** Throughout this work, we use the following Android smartphones:

- OPPO K10 with Dimensity 8000-MAX and Android 12.
- Redmi K50 with Dimensity 8100 and Android 12.
- Xiaomi 9 with Snapdragon 855 and Android 11.
- Xiaomi 9 with Snapdragon 855 and Android 12.

- OnePlus 7Pro with Snapdragon 855 and Android 12.

**System Calls.** We have already analyzed the most vulnerable return values on Android smartphones in Section III, and we choose 5 of them to infer fine-grained use behaviors, where the first three are disclosed in previous work [18], while the last two are discovered in our study:

- `sysinfo.procs`: Number of current processes.
- `statvfs.f_bavail`: Number of free blocks for unprivileged users.
- `sysconf._SC_AVPHYS_PAGES`: Number of currently available pages of physical memory.
- `statvfs.f_ffree`: Number of free inodes.
- `sysinfo.freeram`: Size of available memory.

By default, the return values of the selected system calls are read every 1 ms and collected for 5 seconds.

**Applications.** Several widely used applications are our target applications: Telegram, YouTube, Gmail, and OneNote. And for each application, we choose a set of user behaviors (e.g., sending messages, sending emails) that are more sensitive from the user’s perspective to identify. The list of these applications and user behaviors is shown in Table III.

TABLE III  
DETAILS OF APPLICATIONS AND FINE-GRAINED USER BEHAVIORS IN OUR EXPERIMENTS AND THE ACCURACY OF CLASSIFICATION

Application	User Behavior	Description	Accuracy
Telegram	Launch App	Launch the Telegram application.	0.9855
	View Messages	Open a chat page from the chat list.	
	Send Messages	Send a message to others in a chat.	
	View Profile	Open the user profile page from the menu.	
YouTube	Launch App	Launch the YouTube application.	0.9684
	Refresh Videos	Refresh the video list on the home page.	
	View Videos	Open a video from the video list.	
	Short Videos	Open a short video by tapping the button.	
Gmail	Search Videos	Search videos with keywords.	1.0000
	Launch App	Launch the Gmail application.	
	View Emails	Open an email from the email list.	
	Send Emails	Email a friend or person.	
OneNote	Search Emails	Search emails with keywords.	0.9834
	Launch App	Launch the OneNote application.	
	View Notes	Open a note from the note list.	
	Create Notes	Create a new note and save it.	
All apps	Search Notes	Search notes with keywords.	0.9809
	All behaviors	All applications and all user behaviors.	

**Additional Behaviors.** Besides, we also consider some other user behaviors not included in the above list. Our basic principle is that while the user is operating on the foreground application, there is a high probability that the video or music is playing in the background. Our goal is to identify these two types of behaviors:

- State of the background music (playing).
- State of the PiP hover window (playing, pausing).

**Dataset.** In our dataset, each user behavior is emulated 200 times separately on each experimental device. We first define the user behaviors to be analyzed in our experiments (17 types shown in Table III), then construct the corresponding emulating bot scripts for each user behavior as described in Section IV-D, and use them as a reference to label the time series data collected from victim smartphones. We then shuffle these collected time series data with a one-time generated



random number seed and divide these data into a training and test set in a 7:3 ratio. For 200 time-series data corresponding to each user behavior, we randomly select and insert 140 time-series data into the training set and the remaining 60 into the test set. The data between the training and test sets will not be mixed in our subsequent experiments, i.e., we will never use the data in the test set to train classification models. Then, we use the training set to build the classification models and the test set to evaluate their accuracy.

**Notes.** In our experiments, we only consider a total of 17 user behaviors for 4 applications. So if the user is using another application or performing another behavior not included in our list, the classifier will incorrectly classify it as one of them. However, we do not consider this a significant issue since the inference accuracy is still 0.8911 for 41 user behaviors shown in Section VI-F1. And if the behaviors considered are sufficient to cover the user's daily use, the classifier will not be confused by other behaviors.

### B. Inference Accuracy of Fine-Grained User Behaviors

We first evaluate the accuracy of each application and the fine-grained user behaviors, then analyze all four applications and their user behaviors together. Afterward, we evaluate the accuracy of two additional user behaviors, i.e., the state of the background music and the PiP hover window.

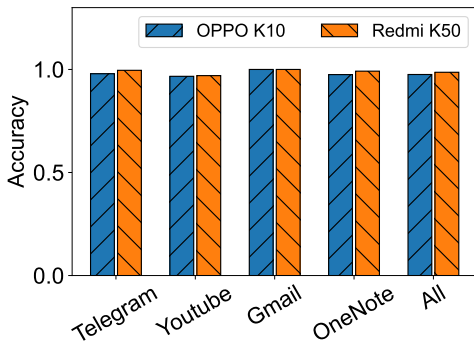


Fig. 7. Accuracy of inferring user behaviors on individual applications and all user behaviors.

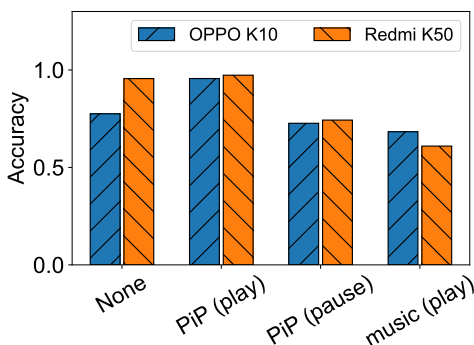


Fig. 8. Accuracy of inferring the state of the background music and the PiP hover window.

**Accuracy of Individual Applications.** First, we evaluate the accuracy of individual applications listed in Table III. The result in Fig. 7 shows that our attack can successfully infer user behaviors on individual applications with an accuracy above 96%. Meanwhile, we can identify the four user behaviors with 100% accuracy for Gmail on both smartphones.

**Accuracy of All User Behaviors.** Second, we combine all the user behaviors into one set, then evaluate the accuracy of this set. Fig. 7 shows that the accuracy of identifying user behaviors from the whole test set (17 different behaviors) can still reach 98% on average.

**Accuracy of Additional Behaviors.** Finally, we evaluate the accuracy of the state of the background music and the state of the PiP hover window. Fig. 8 shows that our attack can successfully infer these two behaviors even when the user is performing other user behaviors on the foreground application, and the accuracy of identifying these states is about 80%.

### C. Evaluation of Impact Factors

1) *Impact of CNN-GRU Network:* To evaluate the impact of our CNN-GRU network on the accuracy of our attack, we first use the DTW-KNN algorithm (with different values of  $K$ ) and the CNN-GRU network to separately classify user behaviors on OPPO K10. We also process the data using the min-max normalization algorithm. As shown in Fig. 9, the accuracy of the CNN-GRU network is 15% higher than the accuracy of the DTW-KNN algorithm with the best  $K$  value (0.9755 for the CNN-GRU network and 0.8510 for the DTW-KNN algorithm). In particular, the gap in accuracy between the two is up to 29% (0.9750 and 0.7542) for OneNote.

Then, we also compare the accuracy of the CNN-GRU network with alone CNN and RNN models. The CNN model used in our experiment is the 1D-CNN network [29], and the RNN model used in our experiment is an LSTM-only network and a GRU-only network. Fig. 10 shows that the accuracy of the CNN-GRU model is 7% higher than the accuracy of the 1D-CNN model (0.9755 and 0.9118), 37% higher than the accuracy of the LSTM model (0.9755 and 0.7137), and 1.5% higher than the accuracy of the GRU model (0.9755 and 0.9608). The result demonstrates that both CNN and RNN models can be used to classify user behaviors, but our CNN-GRU model can achieve the best accuracy.

2) *Impact of Min-Max Normalization:* We evaluate the impact of the min-max normalization algorithm on the accuracy of our attack through:

- Comparing the inference accuracy between normalized data and raw data;
- Comparing the inference accuracy among four different preprocessing algorithms.

And both experiments demonstrate that the min-max normalization algorithm can improve the accuracy of our attack.

First, we use the raw time series data and the min-max normalized data separately to build the classification models using the DTW-KNN algorithm and our CNN-GRU network, then evaluate their accuracy on OPPO K10. The result in Fig. 11 shows that the accuracy of using min-max normalized data is 23% higher than the accuracy of using raw data for

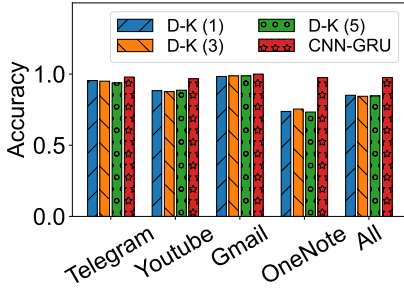


Fig. 9. Accuracy of using CNN-GRU network and DTW-KNN algorithm.

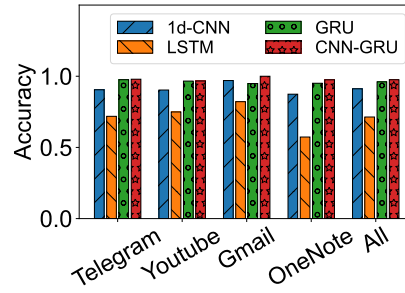


Fig. 10. Accuracy of using different deep learning methods.

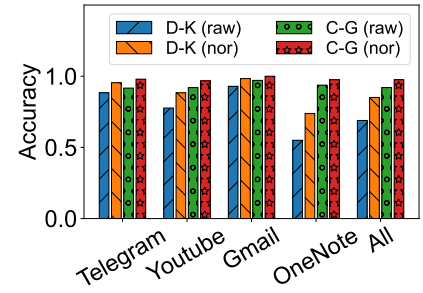


Fig. 11. Accuracy of using min-max normalized data and raw data.

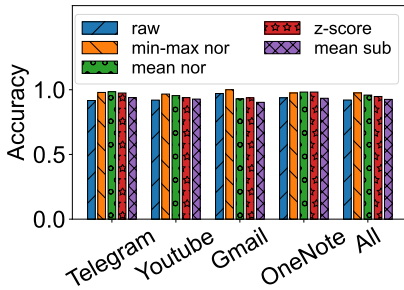


Fig. 12. Accuracy of using different data preprocessing methods.

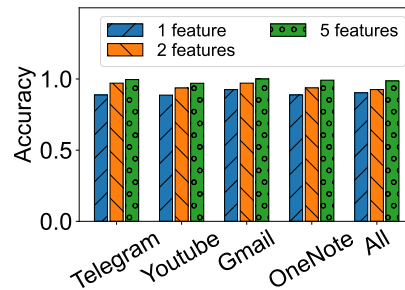


Fig. 13. Accuracy of using different feature dimensions.

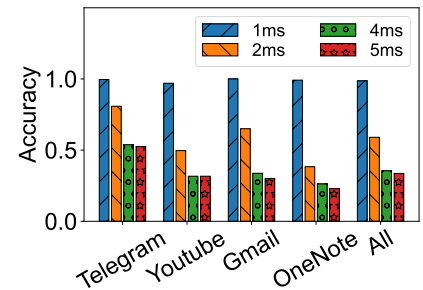


Fig. 14. Accuracy of using different invoking intervals.

the DTW-KNN algorithm (0.6892 for raw data and 0.8510 for min-max normalized data) and 6% higher for the CNN-GRU network (0.9206 for raw data and 0.9755 for min-max normalized data).

Then, we infer the user behaviors using four different data preprocessing methods (min-max normalization, mean normalization, z-score standardization, and mean subtraction) on OPPO K10 with our CNN-GRU network. As shown in Fig. 12, all the preprocessing methods can improve the accuracy of our attack compared with the baseline (0.9206). And the accuracy of using min-max normalization ranks first among all the preprocessing approaches (0.9755), which is 1.7% higher than the accuracy of using mean normalization (0.9588), 2.9% higher than the accuracy of using z-score standardization (0.9480), and 5.4% higher than the accuracy of using mean subtraction (0.9255) on average.

3) *Impact of Feature Dimension*: To evaluate the impact of feature dimension on the accuracy of our attack, we use our CNN-GRU network with different feature dimensions (1, 2, and 5) to classify user behaviors on Redmi K50. And we also use the data preprocessed using the min-max normalization algorithm to evaluate the accuracy. Since there are differences in the consumption of resources such as storage and memory by different user behaviors, and different return values have different preferences for identifying different user behaviors, we select the feature or combination of features with the highest accuracy for feature fusion.

From the result of our experiments shown in Fig. 13, we can see that the more features we use, the higher the accuracy of our attack. When we use only one feature, the accuracy of

our attack is 0.9029, and when we use 5 features, the accuracy of our attack reaches 0.9863, which is 9% higher than the accuracy of using only one feature. Although the model with feature fusion leads to worse results than the model without feature fusion in some cases, the experimental results show that our chosen return values all have a positive effect.

4) *Impact of Invoking Interval*: The speed of invoking system call return values affects the accuracy of identifying user behaviors. To evaluate the impact of the interval of invoking the system call return values, we analyze the accuracy of our attack with different invoking intervals (1ms, 2ms, 4ms, and 5ms) on Redmi K50, and the inference accuracy in these cases is shown in Fig. 14. The accuracy of inferring user behaviors decreases by 40% (from 0.9863 to 0.5902) when the invoking interval increases from 1ms to 2ms, and by 66% (from 0.9863 to 0.3363) when the invoking period increases to 5ms. Therefore, we recommend setting the invoking interval to no more than 2ms for accurate inference.

#### D. Timeliness and Overhead

**Timeliness.** First, we evaluate the timeliness of our attack. In our analysis, we ignore the time delay caused by network transmission and use the time from when the attacker receives the uploaded data from the victim's smartphone to the output of the CNN-GRU classifier as the evaluation metric for timeliness. Fig. 15 shows the time needed to identify 1800 fine-grained user behaviors on OPPO K10. The result demonstrates that the average time is 33.63ms, and over 95% of behaviors can be identified in 40ms.

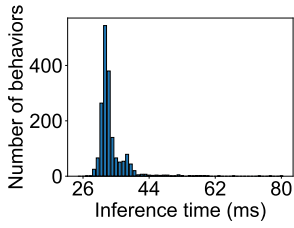


Fig. 15. Timeliness evaluation of our attack.

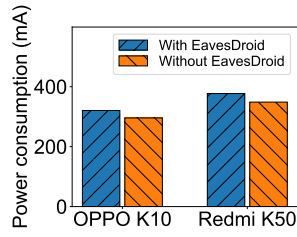


Fig. 16. Power consumption evaluation of our attack.

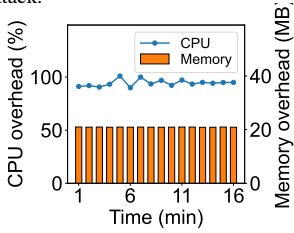


Fig. 17. Computational resource consumption evaluation of our attack.

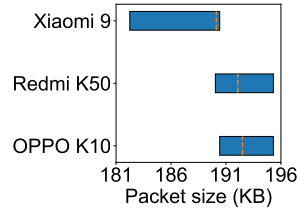


Fig. 18. Network traffic evaluation of our attack.

**Power Consumption.** Next, we evaluate the power consumption of our attack on smartphones. We use AccuBattery to collect the electric current data when the victim's smartphone is idle and when the victim's smartphone is running our attack application. The result shown in Fig. 16 demonstrates that our attack application consumes 8% additional power on average. When the application is not used, the average power consumption is about 322mA, while when it is used, the average power consumption is about 349mA.

**Computational Resource Consumption.** Afterward, we evaluate the computational resource consumption of our attack on the OnePlus 7Pro. In this experiment, we use a monitoring application called Scene, which can read the CPU and memory usage of any running application to evaluate computational resource consumption. We run our attack application on the smartphone for 15 minutes and monitor the CPU and memory usage. As shown in Fig. 17, the average CPU usage is 94.4% on a single core, and the average memory usage is 20.94 MB when using our attack application.

**Traffic Overhead.** Finally, we evaluate the network traffic overhead of our attack by analyzing data uploaded from several smartphones. As shown in Fig. 18, the average packet size is 191.6 KB. The blue bars represent the packet size range on each device, and the orange dashed lines represent the average packet size.

### E. Adaptability of Attack

We evaluate the adaptability of our attack through cross-device experiments and version-drift experiments.

1) *Cross-Device Experiments:* We perform four experiments to evaluate the inference accuracy across different Android device models and versions, and the devices and versions are listed in Table IV. The result shown in Fig. 19 demonstrates that the accuracy of our attack is up to 0.9755 for devices with the same model and the same Android version,

0.8212 for devices with different models and the same Android version, both of which indicate that our attack is adaptable to devices with the same Android version. However, the accuracy of our attack drops to 0.3076 for devices with the same model and different Android versions, 0.2183 for devices with different models and Android versions. Therefore, We cannot successfully launch our attack on devices with different Android versions, and we also find that the same user behavior can cause various return value changes for different Android versions, which may be due to the diverse execution mechanisms of user programs under different Android versions.

TABLE IV  
DEVICE INFORMATION USED TO EVALUATE THE CROSS-DEVICE ADAPTABILITY OF OUR ATTACK AND EVALUATION RESULTS

Device A	Device B	Description	Accuracy
OPPO K10 (Android 12)	OPPO K10 (Android 12)	same model same version	0.9755
Xiaomi 9 (Android 11)	Xiaomi 9 (Android 12)	same model different versions	0.3076
OPPO K10 (Android 12)	Redmi K50 (Android 12)	different models same version	0.8212
Redmi K50 (Android 12)	Xiaomi 9 (Android 11)	different models different versions	0.2183

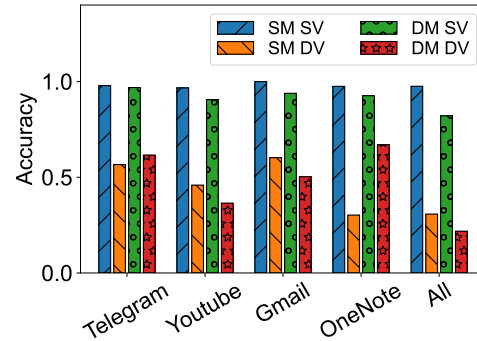


Fig. 19. Cross-device adaptability evaluation of our attack. SM SV: same model and same version; SM DV: same model and different versions; DM SV: different models and same version; DM DV: different models and different versions.

2) *Version-Drift Experiments:* We also evaluate the inference accuracy of our attack on the same application with different versions. The experiment is conducted on Xiaomi 9, and the application versions are listed in Table V. The experimental result shows that our attack can handle the version drift of applications. The inference accuracy of our attack is up to 0.9925 and 0.9825 for each application with the same version, still about 0.8475 and 0.8537 for each application with high version drift. We believe that our attack can handle version drift because the operating logic and UI of applications are relatively stable across different versions.

### F. Evaluation in Complex Scenarios

While our previously emulated behaviors are performed in a less-noisy and controlled environment, these behaviors

TABLE V  
APPLICATION AND VERSION INFORMATION USED TO EVALUATE THE  
VERSION DRIFT OF OUR ATTACK, AND EVALUATION RESULTS

Application	Model Version	Test Version	Accuracy
Telegram	9.0.0	8.7.0	0.8475
		8.8.2	0.8763
		8.9.0	0.9762
		9.0.0	0.9925
Gmail	2022.08.07 (468496502)	2021.09.19 (399766500)	0.8537
		2022.01.09 (422969509)	0.9050
		2022.05.15 (454752110)	0.9287
		2022.08.07 (468496502)	0.9825

can be affected by other factors in the real world, such as other running processes and changes in user behavior patterns (e.g., the varying message length, the varying interval between keyboard input and the press of the send button). Therefore, we also evaluate our attack in more complex scenarios.

1) *Multi-Behavior Traces*: First, when the user uses the smartphone, he/she usually performs a series of behaviors in succession, rather than only a specific behavior during our collection time (5s). Therefore, we evaluate the inference accuracy of our attack on multi-behavior traces on Xiaomi 9.

In our experiment, we set the number of user behaviors in each trace from 1 to 3. There are 17 categories of one-behavior traces, 12 categories of two-behavior traces, and 12 categories of three-behavior traces. The experimental result shows the inference accuracy is about 0.8911 for 41 categories of behavior traces. Among them, the accuracy is 0.8706, 0.9287, and 0.8833 for single behaviors, two-behavior combinations, and three-behavior combinations, which indicates that our attack can be successfully launched with multi-behavior traces.

2) *Noisy Execution Environment*: Second, in our previous experiments, user behaviors are emulated in a comparatively simple environment with only system noise and no additional noise from other processes. However, in real-world situations, many other processes are running in the background that may affect the inference accuracy of our attack. Therefore, we evaluate the robustness of our attack against noisy execution environments by adding additional workloads along with the emulated behaviors on Xiaomi 9.

In our experiment, the number of additional running processes that interfere with our attack ranges from 0 to 3. The result in Fig. 20 demonstrates that our attack is robust against noisy execution environments for the classification model trained with no background noise. The accuracy of our attack is as high as 0.9841 with 0 other running processes and still 0.8653 with one other running process. However, the inference accuracy drops to 0.7350 and 0.6993 when the number of other running processes increases to 2 and 3, respectively, which may challenge the robustness of our attack.

Therefore, to further improve and show the robustness of our

attack, we train another classification model with these noisy data and evaluate the inference accuracy for the whole dataset with 0, 1, 2, and 3 additional running processes. Fig. 21 shows the attack results of our classification model trained on the noisy data, with an inference accuracy of over 97% for 0 and 1 other running processes. While with 2 and 3 other running processes, the inference accuracy drops slightly to 0.9245 and 0.9020, indicating that our attack is still robust to the noisy execution environment when we train the classification model with enough noisy data.

3) *Varied Message Lengths and Operation Intervals*: Third, due to varied message lengths, varied intervals between each keyboard input, and other reasons, user behavior patterns sometimes differ in practical situations. Therefore, we evaluate the inference accuracy of our attack by varying the message length and the operation interval of sending messages on Xiaomi 9. We vary the message length from 1 to 4 characters and the interval between keyboard input, keyboard input and send button press from 0.2s to 1s (0.2s step). As shown in Fig. 22, our attack can still infer the correct user behavior (i.e., input and send messages) from 17 total behaviors with an inference accuracy above 0.9200, indicating that our attack can be successfully launched with varied message lengths and operation intervals.

#### G. Stealthiness of Attack

To evaluate the stealthiness of our attack, we analyze our malicious application through static and run-time malware detection tools.

1) *Static Detection*: We use VirusTotal [33], [34], an online static anti-malware scanning service widely used by researchers and industry practitioners, to scan our attack application. As shown in Fig. 23, our attack application can evade all 65 well-known anti-malware engines on VirusTotal, including Avast, Avira, BitDefender, and other powerful engines.

2) *Run-Time Detection*: Since our malicious application can evade static detection, we evaluate the stealthiness of our attack using dynamic malware detection. Our evaluation shows that our attack can bypass built-in and popular third-party detection tools.

**Built-in Detection.** Most smartphones are only equipped with built-in detection engines provided by Android or their manufacturers. We have successfully launched our attack on OPPO K10, Redmi K50, Xiaomi 9, and OnePlus 7Pro, and the malicious application ran for several hours without being detected on these devices, both of which show that our attack can be effective against widely used Android devices.

**Third-Party Detection.** In addition, we also evaluate the stealthiness of our attack with popular third-party anti-malware engines. We deploy and run our malicious application for several hours on OnePlus 7Pro, which is equipped with Avast, AVG, and Kaspersky. The result shown in Fig. 24 demonstrates that our attack can evade all of these anti-malware engines, highlighting the stealthiness of our attack.

#### H. Evaluation in Real-World Settings

We further evaluate the accuracy of our attack in real-world settings, where users use the smartphone to perform random

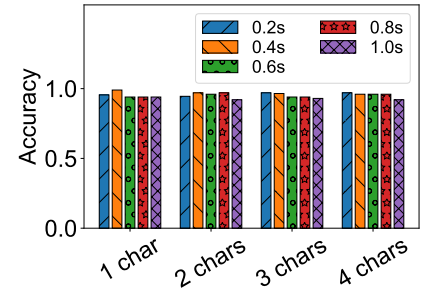
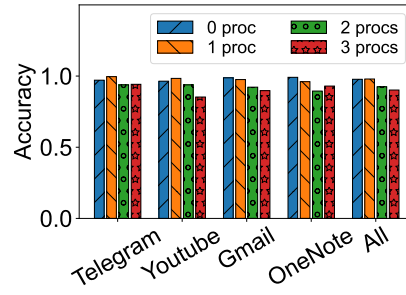
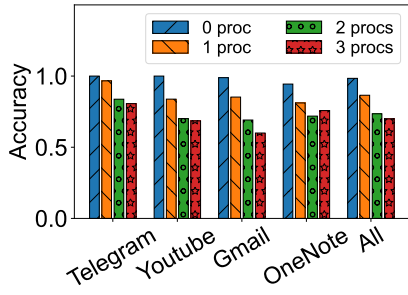


Fig. 20. Evaluation result of our attack in noisy execution scenarios (model without noisy data).

Fig. 21. Evaluation result of our attack in noisy execution scenarios (model with noisy data).

Fig. 22. Evaluation result of our attack against varied message lengths and operation intervals.

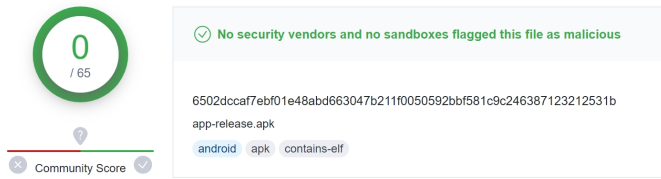


Fig. 23. Stealthiness evaluation with VirusTotal.

behaviors is 86% for all four applications when we use the model trained with noisy data (66% for the model trained without noisy data). The difference in accuracy between these models has similarities to those in the previous experiments shown in Fig. 20 and Fig. 21. The accuracy is slightly reduced compared to the results in Section VI-B but still sufficient to ensure practical inferring with reasonable guesses based on the context of user behaviors.

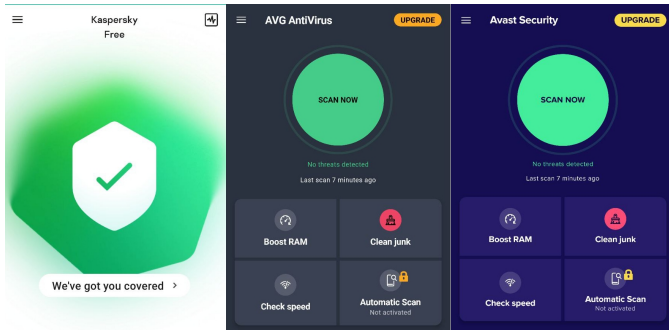


Fig. 24. Stealthiness evaluation with Avast, AVG, and Kaspersky.

user behaviors. In our experiment, 6 users use OPPO K10, Redmi K50, and Xiaomi 9 smartphones. They then perform random fine-grained user behaviors (17 behaviors in total described in Section VI-A) for 2 minutes.

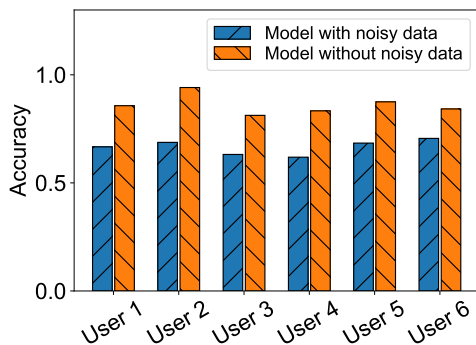


Fig. 25. Accuracy of our attack in real-world settings.

Fig. 25 shows that the average accuracy of inferring user

## VII. MITIGATION AND FUTURE WORK

In this section, we discuss the possible mitigation approaches against the proposed attack and future work.

### A. Mitigation

**Malware Detection.** An intuitive mitigation approach is to rely on malware scanning or on-device malware detection to detect abnormal behaviors in applications, such as frequent system call invocations. However, as we have evaluated, neither the existing static malware detection nor the runtime malware detection can detect the abnormal behaviors of our attack application. On the one hand, since standard Linux system calls are invoked so frequently in normal OS operations, invoking these system calls repeatedly would not be considered abnormal. On the other hand, existing malware detection methods [35] focus more on the permissions of the applications [36], [37] rather than the invocation of system calls, as well as behavior identification and classification [38], [39], which is hard to integrate into Android systems.

**Obfuscation of Return Values.** Another simple mitigation approach is to obfuscate the values of system calls. Obfuscating the return values of system calls can confuse attackers, which can be achieved by running random workloads in the background. However, our attack can identify the state of the background music and the PiP hover window as we have evaluated, which means that these workloads are still observable. Therefore, the main challenge is to determine the appropriate amount of these workloads. On the one hand, excessive workloads would consume system resources and degrade system performance. On the other hand, insufficient workloads would fail to mask user behaviors, allowing attackers still can launch effective attacks.

**Access Control of Return Values.** A more effective and practical approach is to use access control to restrict the permissions of applications. Our idea builds on the Android security model, which uses discretionary access control (DAC) to isolate different applications. Each application on Android can be considered a distinct user since it is assigned a unique Linux UID and GID during installation, and permissions are just strings associated with the application identifiers [40].

Role-based access control (RBAC) is a mechanism that allows users to assign roles to applications and restrict the permissions of applications. Consequently, a viable approach is to use RBAC to manage the permissions of each application, i.e., to prevent applications with no permissions from invoking Linux system calls, while allowing applications with permissions to invoke Linux system calls without restriction.

Android uses security-enhanced Linux (SELinux) to enforce mandatory access control (MAC) on all processes, even those running with root/superuser privileges. With this mechanism, all running applications are assigned roles. Then their access to system resources can be monitored by the SELinux access manager based on the security policy provided by the operating system. Therefore, we could filter suspicious applications that invoke system calls based on a whitelist by adding access rules to the security policy.

### B. Future Work

Some directions for future work include classifying previously unseen user behaviors, launching our attack on Apple devices, and implementing effective mitigations.

**Classifying Previously Unseen Behaviors.** The first limitation of our approach is the use of supervised learning algorithms, which allow the attacker to identify already-known user behaviors in training datasets. However, it is not possible to identify classes of user behaviors that were not trained during the training phase. Therefore, future work may focus on identifying previously unseen applications and user behaviors, which require semi-supervised or unsupervised learning rather than supervised learning.

**Launching Attack on Apple Devices.** The second limitation of our approach is that, like most work, we only focus on inferring user behaviors on Android systems. Therefore, future work could focus more on the iOS mobile operating system to fill the gap with inferring privacy on Apple smartphones with OS side-channel attacks. And the iOS kernel is built on top of Mach and FreeBSD, which is similar to the Linux kernel and has many system calls, so it is possible to launch our attack on Apple devices. And one of the main similarities between iOS and Android is that the control of permissions is limited to access to contacts, access to storage, and other aspects. Therefore, the attack against Android smartphones proposed in this paper is likely to bypass the existing defense mechanisms for user privacy on iOS.

**Implementing Effective Mitigations.** The third limitation of our approach is that we only discuss the potential mitigations against the proposed attack, but we never implement any of them to protect the privacy of user behaviors. Thus, it would be interesting to develop effective malware detection

techniques and implement efficient but not excessive obfuscation or access control mechanisms for vulnerable system calls.

## VIII. CONCLUSION

This paper proposes *EavesDroid*, an OS side-channel attack on Android smartphones that enables unprivileged attackers to infer fine-grained user behaviors. Without requiring additional privileges, *EavesDroid* permits the attacker to identify fine-grained user behaviors with an accuracy rate of 98% in 40ms for the test set and 86% in real-world settings. And we show that our CNN-GRU classifier outperforms the DTW-KNN classifier by about 15%, while mix-max normalization and feature combination can improve the accuracy by about 6% and 9%, respectively. In addition, *EavesDroid* works across a wide range of smartphones running the same version of Android and can evade static and dynamic anti-malware detection, highlighting the vulnerability of our attack and the need for countermeasures. Therefore, we suggest performing effective malware detection, obfuscating vulnerable return values with low overhead, or restricting applications from accessing vulnerable return values to enhance the security of Android smartphones.

## ACKNOWLEDGEMENTS

This work was supported by National Key R&D Program of China under Grant No. 2022YFB3103800 and National Natural Science Foundation of China under Grant Nos. 61972295 and 62072247.

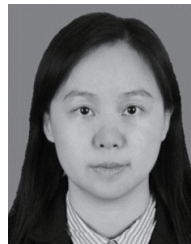
## REFERENCES

- [1] R. Spreitzer, V. Moonsamy, T. Korak, and S. Mangard, "Systematic Classification of Side-Channel Attacks: A Case Study for Mobile Devices," *IEEE Communications Surveys & Tutorials*, vol. 20, no. 1, pp. 465–488, 2017.
- [2] X. Lu, L. Xiao, P. Li, X. Ji, C. Xu, S. Yu, and W. Zhuang, "Reinforcement Learning-Based Physical Cross-Layer Security and Privacy in 6G," *IEEE Communications Surveys & Tutorials*, vol. 25, no. 1, pp. 425–466, 2023.
- [3] D. Wang, A. Neupane, Z. Qian, N. B. Abu-Ghazaleh, S. V. Krishnamurthy, E. J. Colbert, and P. Yu, "Unveiling your keystrokes: A Cache-based Side-channel Attack on Graphics Libraries," in *Network and Distributed Systems Security (NDSS) Symposium 2019*. ISOC, 2019.
- [4] B. Yang, R. Chen, K. Huang, J. Yang, and W. Gao, "Eavesdropping user credentials via GPU side channels on smartphones," in *Proceedings of the 27th ACM International Conference on Architectural Support for Programming Languages and Operating Systems*. ACM, 2022, pp. 285–299.
- [5] H. Ma, J. Tian, D. Gao, and C. Jia, "On the Effectiveness of Using Graphics Interrupt as a Side Channel for User Behavior Snooping," *IEEE Transactions on Dependable and Secure Computing*, vol. 19, no. 5, pp. 3257–3270, 2021.
- [6] M. Gao, Y. Liu, Y. Chen, Y. Li, Z. Ba, X. Xu, and J. Han, "InertiEAR: Automatic and Device-independent IMU-based Eavesdropping on Smartphones," in *IEEE INFOCOM 2022 - IEEE Conference on Computer Communications*. IEEE, 2022, pp. 1129–1138.
- [7] P. Hu, H. Zhuang, P. S. Santhalingam, R. Spolaor, P. Pathak, G. Zhang, and X. Cheng, "AccEar: Accelerometer Acoustic Eavesdropping with Unconstrained Vocabulary," in *2022 IEEE Symposium on Security and Privacy (SP)*. IEEE, 2022, pp. 1757–1773.
- [8] D. Gruss, E. Kraft, T. Tiwari, M. Schwarz, A. Trachtenberg, J. Hennessy, A. Ionescu, and A. Fogh, "Page Cache Attacks," in *Proceedings of the 2019 ACM SIGSAC Conference on Computer and Communications Security*. ACM, 2019, pp. 167–180.

- [9] B. Gulmezoglu, A. Zankl, M. C. Tol, S. Islam, T. Eisenbarth, and B. Sunar, "Undermining User Privacy on Mobile Devices Using AI," in *Proceedings of the 2019 ACM Asia Conference on Computer and Communications Security*. ACM, 2019, pp. 214–227.
- [10] P. Cronin, X. Gao, H. Wang, and C. Cotton, "An Exploration of ARM System-Level Cache and GPU Side Channels," in *Annual Computer Security Applications Conference*. ACM, 2021, pp. 784–795.
- [11] H. Naghibijouybari, A. Neupane, Z. Qian, and N. Abu-Ghazaleh, "Rendered Insecure: GPU Side Channel Attacks are Practical," in *Proceedings of the 2018 ACM SIGSAC Conference on Computer and Communications Security*. ACM, 2018, pp. 2139–2153.
- [12] C. Luo, Y. Fei, and D. Kaeli, "Side-Channel Timing Attack of RSA on a GPU," *ACM Transactions on Architecture and Code Optimization*, vol. 16, no. 3, pp. 1–18, 2019.
- [13] A. R. Javed, M. O. Beg, M. Asim, T. Baker, and A. H. Al-Bayatti, "Alphalogger: Detecting motion-based side-channel attack using smartphone keystrokes," *Journal of Ambient Intelligence and Humanized Computing*, pp. 1–14, 2020.
- [14] R. Spreitzer, G. Palfinger, and S. Mangard, "SCAnDroid: Automated Side-Channel Analysis of Android APIs," in *Proceedings of the 11th ACM Conference on Security & Privacy in Wireless and Mobile Networks*. ACM, 2018, pp. 224–235.
- [15] R. Spreitzer, F. Kirchengast, D. Gruss, and S. Mangard, "ProcHarvester: Fully Automated Analysis of Procs Side-Channel Leaks on Android," in *Proceedings of the 2018 on Asia Conference on Computer and Communications Security*. ACM, 2018, pp. 749–763.
- [16] X. Zhang, X. Wang, X. Bai, Y. Zhang, and X. Wang, "OS-level side channels without procs: Exploring cross-app information leakage on iOS," in *Network and Distributed Systems Security (NDSS) Symposium 2018*. ISOC, 2018.
- [17] L. Yang, Y. Zhi, T. Wei, S. Yu, and J. Ma, "Inference attack in Android Activity based on program fingerprint," *Journal of Network and Computer Applications*, vol. 127, pp. 92–106, 2019.
- [18] V. Brussani, "ASVAAN: Semi-automatic side-channel analysis of Android NDK," *arXiv preprint arXiv:2204.05911*, 2022.
- [19] J. Ren, M. Lindorfer, D. J. Dubois, A. Rao, D. Choffnes, N. Vallina-Rodriguez *et al.*, "Bug Fixes, Improvements, ... and Privacy Leaks," in *Network and Distributed Systems Security (NDSS) Symposium 2018*. ISOC, 2018.
- [20] A. K. Sikder, G. Petracca, H. Aksu, T. Jaeger, and A. S. Ulugac, "A Survey on Sensor-Based Threats and Attacks to Smart Devices and Applications," *IEEE Communications Surveys & Tutorials*, vol. 23, no. 2, pp. 1125–1159, 2021.
- [21] P. Cronin, X. Gao, C. Yang, and H. Wang, "Charger-Surfing: Exploiting a Power Line Side-Channel for Smartphone Information Leakage," in *30th USENIX Security Symposium (USENIX Security 21)*. USENIX Association, 2021, pp. 681–698.
- [22] J. Ren, M. Lindorfer, D. J. Dubois, A. Rao, D. Choffnes, N. Vallina-Rodriguez *et al.*, "GhostTalk: Interactive Attack on Smartphone Voice System Through Power Line," in *Network and Distributed Systems Security (NDSS) Symposium 2022*. ISOC, 2022.
- [23] A. S. La Cour, K. K. Afridi, and G. E. Suh, "Wireless Charging Power Side-Channel Attacks," in *Proceedings of the 2021 ACM SIGSAC Conference on Computer and Communications Security*. ACM, 2021, pp. 651–665.
- [24] "sysinfo(2) — Linux manual page," The Linux Foundation, 2023. [Online]. Available: <https://man7.org/linux/man-pages/man2/sysinfo.2.html>
- [25] G. Menghani, "Efficient Deep Learning: A Survey on Making Deep Learning Models Smaller, Faster, and Better," *ACM Computing Surveys*, vol. 55, no. 12, pp. 1–37, 2023.
- [26] S. Dong, P. Wang, and K. Abbas, "A survey on deep learning and its applications," *Computer Science Review*, vol. 40, p. 100379, 2021.
- [27] M. Tan and Q. Le, "EfficientNet: Rethinking Model Scaling for Convolutional Neural Networks," in *Proceedings of the 36th International Conference on Machine Learning*. PMLR, 2019, pp. 6105–6114.
- [28] H. Ismail Fawaz, G. Forestier, J. Weber, L. Idoumghar, and P.-A. Muller, "Deep learning for time series classification: a review," *Data Mining and Knowledge Discovery*, vol. 33, pp. 917–963, 2019.
- [29] W. Tang, G. Long, L. Liu, T. Zhou, J. Jiang, and M. Blumenstein, "Rethinking 1D-CNN for Time Series Classification: A Stronger Baseline," *arXiv preprint arXiv:2002.10061*, 2020.
- [30] W. Chen and K. Shi, "Multi-scale Attention Convolutional Neural Network for time series classification," *Neural Networks*, vol. 136, pp. 126–140, 2021.
- [31] L. Xie and A. Yuille, "Genetic CNN," in *2017 IEEE International Conference on Computer Vision (ICCV)*. IEEE, 2017, pp. 1379–1388.
- [32] R. Fu, Z. Zhang, and L. Li, "Using LSTM and GRU neural network methods for traffic flow prediction," in *2016 31st Youth Academic Annual Conference of Chinese Association of Automation (YAC)*. IEEE, 2016, pp. 324–328.
- [33] S. Zhu, Z. Zhang, L. Yang, L. Song, and G. Wang, "Benchmarking Label Dynamics of VirusTotal Engines," in *Proceedings of the 2020 ACM SIGSAC Conference on Computer and Communications Security*. ACM, 2020, pp. 2081–2083.
- [34] S. Zhu, J. Shi, L. Yang, B. Qin, Z. Zhang, L. Song, and G. Wang, "Measuring and Modeling the Label Dynamics of Online Anti-Malware Engines," in *29th USENIX Security Symposium (USENIX Security 20)*. USENIX Association, 2020, pp. 2361–2378.
- [35] J. Qiu, J. Zhang, W. Luo, L. Pan, S. Nepal, and Y. Xiang, "A Survey of Android Malware Detection with Deep Neural Models," *ACM Computing Surveys*, vol. 53, no. 6, pp. 1–36, 2020.
- [36] A. Arora, S. K. Peddoju, and M. Conti, "PermPair: Android Malware Detection Using Permission Pairs," *IEEE Transactions on Information Forensics and Security*, vol. 15, pp. 1968–1982, 2019.
- [37] H.-j. Zhu, W. Gu, L.-m. Wang, Z.-c. Xu, and V. S. Sheng, "Android malware detection based on multi-head squeeze-and-excitation residual network," *Expert Systems with Applications*, vol. 212, p. 118705, 2023.
- [38] T. Lei, Z. Qin, Z. Wang, Q. Li, and D. Ye, "EveDroid: Event-Aware Android Malware Detection Against Model Degrading for IoT Devices," *IEEE Internet of Things Journal*, vol. 6, no. 4, pp. 6668–6680, 2019.
- [39] A. Guerra-Manzanares, M. Luckner, and H. Bahsi, "Concept drift and cross-device behavior: Challenges and implications for effective android malware detection," *Computers & Security*, vol. 120, p. 102757, 2022.
- [40] M. Backes, S. Bugiel, E. Derr, P. McDaniel, D. Octeau, and S. Weisgerber, "On Demystifying the Android Application Framework: Re-Visiting Android Permission Specification Analysis," in *25th USENIX Security Symposium (USENIX Security 16)*. USENIX Association, 2016, pp. 1101–1118.



**Quancheng Wang** was born in 1999. He received the B.S. degree in Software Engineering from Shandong University, Jinan, China, in 2021. He is currently working on his Ph.D. degree at School of Cyber Science and Engineering, Wuhan University, China. His research interests include hardware security, microarchitecture security, and system security.



**Ming Tang** was born in 1976. She received the Ph.D. in School of Computer from Wuhan University, China, in 2007. Currently, she is a professor at the School of Cyber Science and Engineering, Wuhan University, China. Her interests include cryptography, secure design of cryptography chips, lightweight countermeasures against side-channel analysis, and systematic research on side-channel analysis.



**Jianming Fu** received the PhD degree from Wuhan University, Wuhan, China, in 2000. He is currently a professor with the School of Cyber Science and Engineering, Wuhan University. His research interests include system security, software security, mobile security and AI security.